PENNSTATE

MEMS

MECHATRONICS RESEARCH LAB

Clapping Wing Nano Air Vehicles Using Piezoelectric T-beam Actuators

K. Mateti[1], H. K. R. Kommepalli[2], S. Tadigadapa[1], C. D. Rahn[2]
[1]Department of Electrical Engineering,
[2]Department of Mechanical Engineering,
Pennsylvania State University, Univeristy Park, 16802

Background

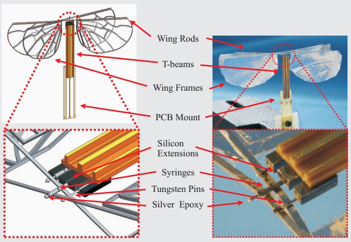

Figure 1: Conceptual drawing of NAV (left) and fabricated device (right)

Nano air vehicles are defined as having wingspans less than 7.5 cm and weighing less than 10 g. Flapping wing NAVs can provide superior indoor mobility for reconnaissance, search and rescue, and hazardous environment exploration. Clapping wing air vehicles are inspired by the Weis-Fogh clap and fling mechanism used by certain insects, where opposing wings almost touch during part of the flap cycle, spawning vortex structures that increase thrust.

All four-winged 'X' type clapping designs however, use electromagnetic motors, gears, linkages and crank-rocker mechanisms, that are difficult to fabricate and have poor efficiency at the sub-millimeter scale.Piezoelectric actuators, however, are attractive because they have high power density, and high efficiency.This research presents the first piezoelectrically driven four winged clapping wing nano air vehicle.

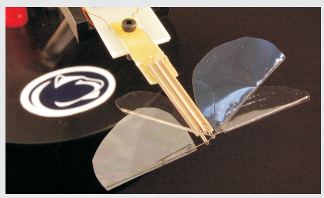

Figure 2: Early prototype of a four winged clapping nano air vehicle

Fabrication

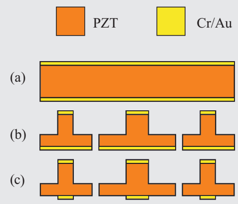

Figure 6: Fabrication process for T-beam actuators photolithography patterns bottom electrode

(a)T-beams are fabricated from bulk 1mm thick PZT-5H (b) a high precision dicing saw machines the PZT (c) photolithography patterns bottom electrodes

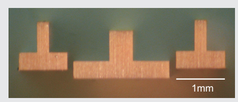

Figure 9: End view of fabricated T-beams

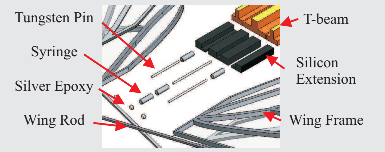

Figure 7: Exploded view of NAV stroke amplification system

162.5 μm tungsten pins and 1 mm x 29 AWG medical syringes form revolute joints. These bond to Si extensions using silver epoxy which then bond to the T-beams using cyanoacrylate . Silver epoxy beads form load bearings which pull the NAV. Wings bond to the ends of the tungsten pins using two part epoxy.

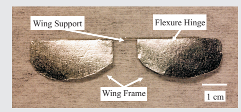

Figure 8: Photograph of fabricated wings

Flexure hinges are created by spacing a 6 cm x 200 μm x 600 μm stainless steel wing support and 100 μm Al foil wing frame 150 μm apart on stretched 12.5 μm thick mylar sheets. Wings are cut and bond to the stroke amplification mechanism shown in figure 7.

Design

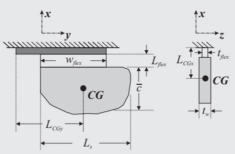

Figure 3: Schematic of the flexure hinge, leading edge, and wing frame. L_{flex}, L_{CG_x} and t_{flex} are key design parameters for wing rotation

Wing rotation is crucial to produce lift. A flexure hinge in the wing allows passive wing rotation during the flap cycle. To ensure proper wing trajectory, the rotational inertia and stiffness of the flexure must be designed properly with respect to the flapping frequency.

$$k_{flex} = \frac{E_w w_{flex} t_w^3}{12 L_{flex}}$$

$$m_{eff} = m_f + m_{aero} = m_f + \frac{\pi \rho \bar{c}^2}{4} L_s$$

$$J_{wing_y} = (m_{eff})(\frac{\bar{c}^2}{12} + L_{CG_x}^2)$$

$$f_R = \frac{1}{2\pi}\sqrt{\frac{k_{flex}}{J_{wing_y}}}$$

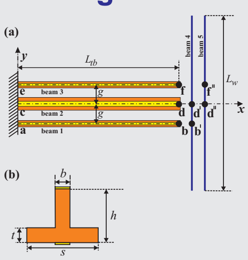

Figure 4: Schematic diagram of the NAV model: (a) top view, and (b) cross-section of a T-beam actuator. Beam 4 is connected to beams 1 and 2 with hinges at b-b' and d-d' and beam 5 is hinged to T-beams 2 and 3 at d-d" and f-f".

T-beam actuators bend upwards when an electric field is applied in the direction of poling. Optimized the small displacement of the T-beams are amplified by a stroke amplification mechanism. The flapping stroke is given by

$$\theta = 2\,tan^{-1}(\delta/g) \approx 2\delta/g$$

where, δ is the T-beam displacement and, g is the clearance between hinges.

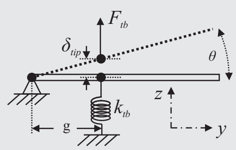

Figure 5: Schematic diagram stroke amplification mechanism, where δ_{tip}, F_{tb}, k_{tb} are the displacement, force, and stiffness of the T-beam, g is the clearance between the two hinges, and $\theta = 2\delta_{tip}/g$, a key design parameter

Lift is proportional to tip velocity, wing stroke amplitude, and wing area. The flapping resonance frequency is maximized while maintaining a stroke amplitude. This is tuned by designing the rotational inertia of the wing, stiffness of the T-beam and gap clearance.

$$k_{tb} = \frac{6 E_{PZT} I_{tb}}{L_{tb}^2 (2L_{tb} + L_{pin})}$$

$$J_{wing_x} = \frac{m_r L_r^2}{12} + 2m_{eff}(\frac{L_s^2}{12} + L_{CG_y}^2)$$

$$f_s = \frac{1}{2\pi} g \sqrt{\frac{k_{tb}}{J_{wing_x}}}.$$

Testing

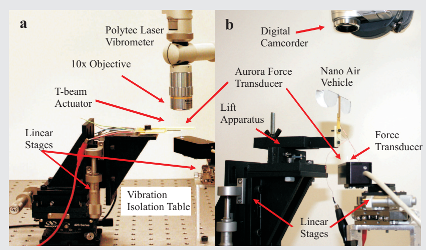

Figure 10: (a) Experimental setup for T-beam actuator displacement and blocking force measurement (b) experimental setup for NAV video and lift measurement

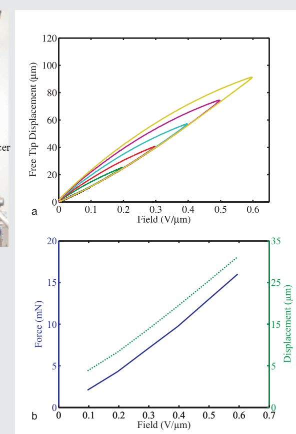

Figure 11: (a) T-beam tip displacement in response to a quasi-static (1Hz) applied electric field (b) measured force of T-beam (left) and corresponding T-beam displacement at the base, due to insufficient clamping

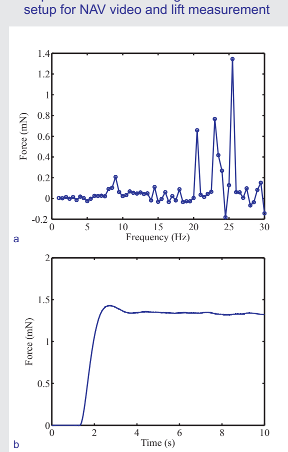

Figure 12: (a) Average lift force versus frequency of NAV in response to a sinusoidal applied field with amplitude 0.7 V/μm with 0.1 V/μm DC bias and (b) low-pass filtered time signal of lift force at 25.5Hz

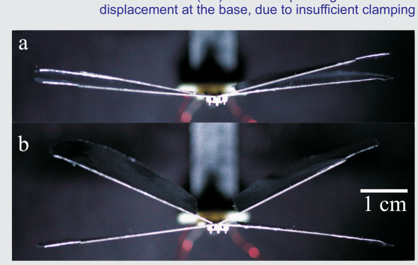

Figure 13: (a) NAV in the closed position (b) NAV in the open position showing ~30 degrees of flapping rotation in response to a sinusoidal applied field with amplitude 0.7 V/μm with 0.1 V/μm DC bias and frequency range from DC to ~9.5Hz

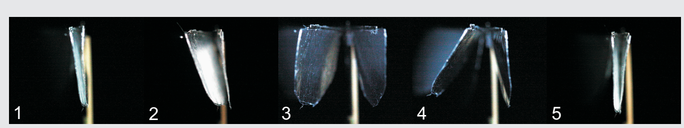

Figure 14: Five strobed photographs at different stages of a flapping cycle, showing ~30 degrees of passive wing rotation allowed by the flexure hinge, in response to a sinusoidal applied field with amplitude 0.7 V/μm with 0.1 V/μm DC bias at 9Hz

Conclusion

A novel mechanism for producing clapping wing motions in a four winged NAV using piezoelectric T-beam actuators has been designed, fabricated and tested. Stroke amplitude of ~30° is obtained at 9Hz with 0.7 V/μm and 0.1 V/m DC bias. Flexure hinges on the wing allow ~30° of passive rotation during the flap cycle. The NAV produced 1.34 mN of thrust at 25.5 Hz.

Future work

To improve lift, rotation and flapping frequency must be predictable and increased. In the next design iteration, a MEMS wing process will be designed to reduce effective mass of the wing frame and ensure precise flexure length. Rigid glass mounting and carbon fiber center beams will improved boundary conditions.

Acknowledgements

This work is supported by the Air Force Office of Scientific Research under grant #FA9550-07-1-0367